Propagation of localized structures in relativistic magnetized electron-positron plasmas using particle-in-cell simulations

Rodrigo A. López, Víctor Muñoz, Adolfo F. Viñas, and Juan A. Valdivia

Citation: Physics of Plasmas **22**, 092115 (2015); doi: 10.1063/1.4930266
View online: http://dx.doi.org/10.1063/1.4930266
View Table of Contents: http://scitation.aip.org/content/aip/journal/pop/22/9?ver=pdfcov
Published by the AIP Publishing

Propagation of localized structures in relativistic magnetized electron-positron plasmas using particle-in-cell simulations

Rodrigo A. López,[1] Víctor Muñoz,[2] Adolfo F. Viñas,[3] and Juan A. Valdivia[2,4]
[1]*Departamento de Física, Facultad de Ciencias Físicas y Matemáticas, Universidad de Concepción, Concepción 4070386, Chile*
[2]*Departamento de Física, Facultad de Ciencias, Universidad de Chile, Casilla 653, Santiago, Chile*
[3]*Geospace Physics Laboratory, Heliophysics Science Division, NASA Goddard Space Flight Center, Greenbelt, Maryland 20771, USA*
[4]*Centro para el Desarrollo de la Nanociencia y la Nanotecnología (CEDENNA), Santiago 9170124, Chile*

(Received 18 May 2015; accepted 21 August 2015; published online 15 September 2015)

We use a particle-in-cell simulation to study the propagation of localized structures in a magnetized electron-positron plasma with relativistic finite temperature. We use as initial condition for the simulation an envelope soliton solution of the nonlinear Schrödinger equation, derived from the relativistic two fluid equations in the strongly magnetized limit. This envelope soliton turns out not to be a stable solution for the simulation and splits in two localized structures propagating in opposite directions. However, these two localized structures exhibit a soliton-like behavior, as they keep their profile after they collide with each other due to the periodic boundary conditions. We also observe the formation of localized structures in the evolution of a spatially uniform circularly polarized Alfvén wave. In both cases, the localized structures propagate with an amplitude independent velocity. © *2015 AIP Publishing LLC*. [http://dx.doi.org/10.1063/1.4930266]

I. INTRODUCTION

The study of wave propagation in relativistic electron-positron plasmas is of importance to understand various processes that take place in several environments such as accretion disks,[1–3] pulsar magnetospheres,[4,5] early universe,[6,7] ultra-intense lasers,[8,9] and laboratory and tokamak plasmas,[10,11] among others. Relativistic effects introduce several sources of nonlinearity, which must be considered to properly model the plasma in these cases: large quiver velocities of particles in the wave field; very large temperatures; and large wave amplitudes. These nonlinear effects modify the propagation characteristics of electrostatic and electromagnetic waves. A number of authors have studied the nonlinear wave propagation in relativistic plasmas. In the unmagnetized case, Chian and Kennel[12] studied the self-modulation instability of strong electromagnetic waves in electron-positron plasmas, excited by the mass variation of particles induced by the wave intensity. This instability can give rise to soliton solutions, which has been proposed as a mechanism to explain the microstructure of pulsar radio pulses. Multiple discussions about the existence of electrostatic solitons in unmagnetized pair plasmas have been carried out in the recent years.[13,14] Numerical simulations have been used as a tool to study the soliton formation and propagation in unmagnetized electron-ion plasmas with particle-in-cell (PIC)[15,16] and Vlasov codes.[17] The same techniques have been used to analyze the evolution of electrostatic solitons in unmagnetized pair plasmas.[18–20]

It is important to mention that in many astrophysical and laboratory settings, where we have relativistic electron-positron plasmas, the presence of the magnetic field is fundamental for their evolution. Hence, several authors have improved the model proposed by Chian and Kennel[12] to include effects that were not considered originally as, the presence of external magnetic fields, ponderomotive force, or ions species, among others.[21–25] In particular, for weakly and strongly magnetized plasmas, it has been shown that the necessary condition for the existence of a modulational instability and the appearance of soliton solutions is fulfilled.[26,27] In these papers, Asenjo *et al.*[26] and López *et al.*[27] studied the self-modulation of a nonlinear Alfvén wave propagating along an ambient magnetic field in a weakly and strongly magnetized electron-positron plasma with fully relativistic temperatures, respectively. Nonlinear Schrödinger (NLS) equations were derived, which produces either a propagating wave train or an envelope soliton, depending on initial conditions. All of this in the context of a relativistic two fluid model. Hence, these soliton solutions are obtained from an approximation to the two fluid relativistic theory, but it remained to be seen if they survive in a fully nonlinear kinetic treatment. One of the aims of this paper is to study the existence of electromagnetic localized structures in relativistic magnetized thermal pair plasmas by using a fully relativistic PIC simulation. In this respect, we will see below that the long term evolution of an initial condition composed of a spatially uniform large amplitude circularly polarized wave will naturally evolve into propagating localized structures that resemble solitons. Hence, it becomes natural to study the stability and spatio-temporal evolution of the two fluid soliton solution for strongly magnetized plasmas found in Ref. 27, using it as initial condition for fields and particle velocities in a PIC simulation. Although we do not in general expect that this solution will be a perfect solitary wave in the PIC simulation because it corresponds to a solution of a two fluid relativistic thermal plasma model, it does give a simple initial condition with which we can start the simulation to

check if these localized structures evolve as such, as was done previously with MHD[28] and hybrid[29] codes. The PIC simulation we use in the current manuscript was previously used to study the parametric decays of a circularly polarized wave, the linear dispersion relation, and the thermally induced electromagnetic fluctuations in relativistic electron-positron plasmas,[30–32] showing a very good agreement between theory and simulation results. We will show that, as expected, the two-fluid soliton solutions do not behave as such in a fully relativistic PIC simulation. However, when the two-fluid solitons are used as an initial condition for the PIC simulation, they do evolve into localized stable structures that have many of the soliton properties. In this manuscript, we characterize the properties of these localized solitary structures that are fully nonlinear solutions to the fully relativistic PIC simulation.

We concentrate on relativistic electron-positron plasmas with finite temperature, to study situations where relativistic effects under strong magnetic fields are relevant, such as the propagation of radio emissions through pulsar magnetospheres,[5] the bulk acceleration or relativistic jets,[33] or the emissions in quasar relativistic jets,[34] among others.

This paper is organized as follows. In Sec. II, the circularly polarized wave and the envelope soliton solution of the nonlinear Schrödinger equation in a strongly magnetized electron-positron plasma, derived in Ref. 27, are presented. In Sec. III, the particle-in-cell simulation is described. In Sec. IV, we study the propagation of a circularly polarized electromagnetic wave and in Sec. V we study the propagation of the envelope soliton. Finally, in Sec. VI, our results are summarized.

II. SOLITON TWO FLUID SOLUTION

Using a relativistic two fluid model, Asenjo *et al.*[35] studied the evolution of a circularly polarized wave propagating along a constant background magnetic field in an electron-positron plasma, given by

$$\vec{A} = a_0[\cos(kz-\omega t)\hat{x} + \sin(kz-\omega t)\hat{y}], \tag{1}$$

where $\vec{A}$ is the vector potential and $a_0 = |A|$ is its amplitude, ω is the frequency, and k is the wave number. The background magnetic field is set in the $\hat{z}$ direction. In Ref. 35, the exact dispersion relation for this circularly polarized wave was calculated, obtaining

$$\omega^2 - c^2k^2 = -\frac{\omega_{pe}^2}{c\sqrt{\lambda}a_0}(v_p - v_e), \tag{2}$$

where the purely transverse velocities induced by the wave are

$$\frac{v_j}{c} = \eta_j \frac{ea_0}{mc^2}\left(\frac{\omega}{f_j\gamma_j\omega + \eta_j\Omega_c}\right)e^{i(kz-\omega t)}. \tag{3}$$

Here, j is the species index ($j=e$ for electrons and $j=p$ for positrons); $\eta_e = 1$; $\eta_p = -1$; $\omega_{pe} = \sqrt{4\pi ne^2/m}$ and $\Omega_c = eB_0/(mc)$ are the plasma and cyclotron frequencies, respectively; n is the number density; e is the positron charge; m is the electron mass; and B_0 is the background magnetic field. $\lambda = e^2/(m^2c^4)$; $\gamma_j = (1 - v_j^2/c^2)^{-1/2}$ is the relativistic Lorentz factor; f is a thermal factor for a relativistic thermal ideal gas, which is related to the temperature by $f = K_3(\mu)/K_2(\mu)$,[36] where $\mu = mc^2/k_BT$; T is the plasma temperature; and K_2 and K_3 are the modified Bessel functions of order 2 and 3, respectively. The dispersion relation is obtained by solving Eqs. (2) and (3) simultaneously. Two branches can be obtained from this dispersion relation, the electromagnetic ordinary branch and the Alfvén branch.

In Ref. 37, the parametric decays for this circularly wave were studied. Various types of instabilities were described, namely, decay, beat, and modulational. In Ref. 27, the modulational instability of an Alfvén wave was studied in the strongly magnetized limit. This limit is characterized by the low-frequency regime $\omega \ll \Omega_c$. In this limit, the purely transverse velocities of Eq. (3) become

$$\frac{v_j}{c} = \sqrt{\lambda}a_0\frac{\omega}{\Omega_c}\left[1 - \left(\eta_j + \frac{f\omega}{\Omega_c}\right)\frac{f\omega}{\Omega_c}\right] - \frac{\eta_j}{2}a_0 f\left(2f^2 + \lambda a_0^2\right)\frac{\omega^4}{\Omega_c^4} + \sqrt{\lambda}a_0 f^2\left(f^2 + 2\lambda a_0^2\right)\frac{\omega^5}{\Omega_c^5}. \tag{4}$$

Using these velocities, the dispersion relation for the strongly magnetized limit is

$$\omega^2 - c^2k^2 + \frac{\omega_{pe}^2}{\Omega_c^2}f\omega^2\left[2 + \frac{\omega^2}{\Omega_c^2}\left(2f + \lambda a_0^2\right)\right] = 0. \tag{5}$$

The modulational instability in the strongly magnetized limit was studied by means of a nonlinear Schrödinger equation, showing that the necessary condition for a modulational instability is fulfilled.[27] This modulational instability admits an envelope soliton solution of the form

$$a(z,t) = a_0\,\mathrm{sech}\left[\sqrt{\frac{Qa_0^2}{2P}}(z - Vt)\right]e^{i\eta}, \tag{6}$$

where

$$P(\omega) = \frac{c^2}{2\omega}, \tag{7}$$

$$Q(\omega) = \frac{\omega_{pe}^2}{4\Omega_c^4}f\lambda\omega^3, \tag{8}$$

and

$$\eta = \frac{V}{2P}z - \left(\frac{V^2}{4P} + \frac{Qa_0^2}{2}\right)t.$$

Here, V is the effective group velocity of the wave packet.[38] The total vector potential is written as

$$\vec{A} = \frac{1}{2}\left[a(z,t)e^{-i\omega t}\hat{h} + a(z,t)^*e^{i\omega t}\hat{h}^*\right], \tag{9}$$

where $\hat{h} = (\hat{x} - i\hat{y})/\sqrt{2}$, and the $*$ corresponds to a complex conjugate quantity. Hence, the electromagnetic wave corresponds to a left-handed circularly polarized wave packet

described by Eq. (6), which propagates with velocity V. For a detailed derivation, see Ref. 27. We will use this soliton solution as an initial condition in the PIC code described below.

III. PARTICLE-IN-CELL SIMULATION

We perform a one dimensional relativistic full electromagnetic particle-in-cell simulation, in which we follow the trajectories of a large group of macroparticles by solving the relativistic equations of motion

$$\frac{d\vec{u}}{dt} = \frac{q}{m}\left(\vec{E} + \frac{\vec{u}}{\gamma c} \times \vec{B}\right), \tag{10}$$

$$\frac{d\vec{x}}{dt} = \frac{\vec{u}}{\gamma}, \tag{11}$$

where $\vec{u} = \gamma\vec{v}$ is the relativistic momentum per unit mass, $\gamma = (1 + |\vec{u}|^2/c^2)^{1/2}$ is the relativistic Lorentz factor, and $\vec{E}$ and $\vec{B}$ are the electric and magnetic fields. We solve the momentum equation of both electrons and positrons in a consistent manner with the electromagnetic fields obtained from Maxwell's equations. Relativistic effects have been included in the Lorentz equation for the particle momentum, Eq. (10), and in their thermal motion, by considering a Maxwell-Jüttner velocity distribution function for the initial condition[39]

$$f(u) = \frac{\mu}{c^3 K_2(\mu)} \exp\left(-\mu\sqrt{1 + \frac{u^2}{c^2}}\right). \tag{12}$$

As explained below, an additional Lorenz boost must be applied to introduce the bulk motion in the particle velocities. We have used a leapfrog scheme for the temporal advance of the motion equations, which are solved using the relativistic version of the Boris-Bunemman method.[40–44] The electromagnetic fields are solved using a standard finite difference method and advanced using a leapfrog scheme.[42] We use a standard quadratic scheme, as described in Ref. 41, to interpolate the initial bulk velocities at the particle position. The same scheme is used to interpolate the fields, and hence the forces, at the particle position, and the contribution of the particles to the charge and current densities at the grid points. We also have implemented a correction to the longitudinal electric field based on Marder[45] and Langdon.[46]

The simulation has only one spatial dimension z and three velocity dimensions are retained. The spatial boundary conditions are periodic and we set the background magnetic field B_0 in the z direction. The system spatial size is $L = 1024\omega_{pe}/c$, the number of spatial grid points is $n_g = 4096$, and the time step used is $\omega_{pe}\Delta t = 0.01$. We have used 1000 particles of each species per grid cell. The same simulation code has been used in the previous papers to describe the parametric decays,[30] the normal modes,[31] and the thermally induced fluctuations[32] in magnetized relativistic pair plasmas with finite temperatures. Good agreement has been shown to occur between the analytical theories and particle simulations.

IV. CIRCULARLY POLARIZED PUMP WAVE

In this section, we show the long term evolution of a left-handed circularly polarized electromagnetic Alfvén wave by means of the fully relativistic PIC simulation described in Sec. III. We start with the vector potential given by Eq. (1) to set the initial condition for the electric and magnetic fields at each point in the grid. Frequency and wave number are obtained from the dispersion relation (2), and the spatially dependent bulk velocities are set from Eq. (3), which are then interpolated to the actual positions of the particles by using the quadratic interpolation scheme described above. The normalized wave number of the pump wave is set to $ck_0/\Omega_c = 0.49$ and the normalized frequency of the pump wave, obtained by solving the dispersion relation (2), is $\omega/\Omega_c = 0.27$. We also add a relativistic thermal velocity for the particles, using a Lorentz transformation for the addition of velocities, obtained from a Maxwell-Jüttner distribution, Eq. (12), with $\mu = 100$.[39]

This same configuration for the initial condition was used in Ref. 30 to study the parametric decays of this wave. In that reference, it is shown that, for $\mu = 100$ and $\sqrt{\lambda}a_0 = 0.2$, this left-handed circularly polarized wave propagates parallel to the background magnetic field as expected. Daughter waves from parametric processes begin to grow at around $\omega_{pe}t \approx 400$, consistent with the linear analysis of Ref. 37. The growth rates of the parametric instabilities increase as the amplitude of the pump wave is increased, and for larger growth rates these instabilities grow at earlier times. In order to study the long term nonlinear evolution of the pump wave described before, we set a relatively large amplitude pump wave to $\sqrt{\lambda}a_0 = 0.5$. With this amplitude, the growth of daughter waves starts very early in the simulation and the parametric stage lasts for a short period, leading to a fully nonlinear regime. Fig. 1 shows the spatio-temporal evolution of the transverse magnetic fluctuations. We observe that at $\omega_{pe}t = 0$ the simulation starts with a spatially uniform amplitude pump wave and at a very early time, $\omega_{pe}t \approx 100$, waves propagating antiparallel to the background magnetic field begin to grow. As the simulation evolves, the nonlinear effects become relevant and these antiparallel waves form localized pulses around $\omega_{pe}t \approx 300$.

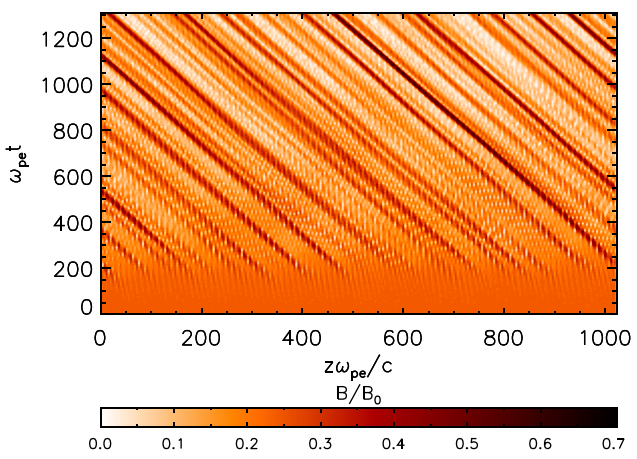

FIG. 1. Spatio-temporal evolution of the transverse magnetic field for $\sqrt{\lambda}a_0 = 0.5$, $\alpha = 1$, and $\mu = 100$.

It becomes clear that these pulses, which have different amplitudes, propagate with the same and constant velocity, $v_p/c \approx 0.53$, which is already a non-intuitive result, since it is expected, following our intuition about the NLS solitons, that the velocity should be amplitude dependent.[47]

In Fig. 2, we show the spatial profile of the transverse magnetic field for three different times. As mentioned before, for $\omega_{pe}t = 0$, we observe the spatially uniform amplitude for the magnetic field in Fig. 2(a). Here, the dotted-blue and dashed-red lines represent the B_x and B_y components of the magnetic field, respectively. Figure 2(b) shows $\omega_{pe}t = 1000$, once the nonlinear effects are dominant and the localized solutions have appeared. Here, we have labeled some localized peaks in the magnetic field, which satisfy the condition $B/B_0 > 0.45$. By comparing Figs. 2(b) and 2(c), all the localized structures propagate at constant velocity, independent of their amplitude, as the distance between the localized structures remains constant, maintaining their spatial profile. This result shows that instabilities and nonlinear effects cause the spatially uniform circularly polarized wave to evolve as localized structures in the long-term behavior of the plasma. Furthermore, it becomes of interest to study the evolution of these localized structures at the individual level.

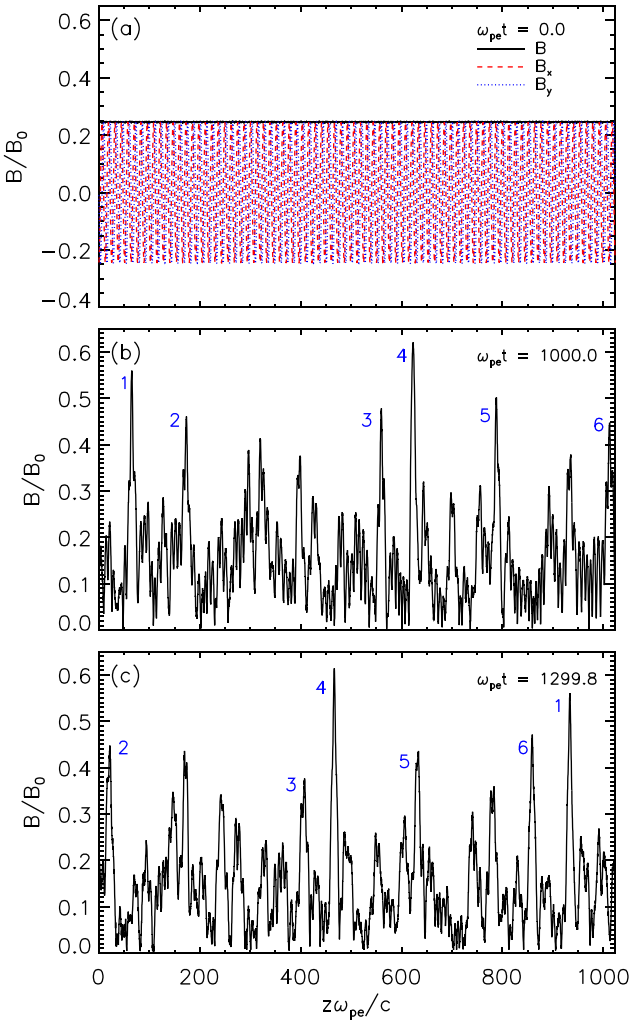

FIG. 2. Transverse magnetic field for $\sqrt{\lambda}a_0 = 0.5$, $\alpha = 1$, and $\mu = 100$. (a) $\omega_{pe}t = 0$, (b) $\omega_{pe}t = 1000$, (c) $\omega_{pe}t = 1299.8$.

V. TWO FLUID SOLITON INITIAL CONDITION

In Section IV, we studied the evolution of the circularly polarized wave described by Eqs. (1)–(3). We observed that the instabilities and nonlinear effects lead to the formation of localized structures in the long term evolution of the simulation. In Ref. 27, the nonlinear evolution of this circularly polarized wave, in the two fluid approximation, is studied in the strongly magnetized regime. Taking a slowly time-varying modulation of the wave envelope, a nonlinear Schrödinger equation was derived and a soliton solution was found, as described in Sec. II. In order to study the fully kinetic evolution of an initial two fluid soliton found in Ref. 27, we set initial conditions of the simulation with the definitions of Sec. II. The normalized amplitude used for the vector potential is $\sqrt{\lambda}a_0 = ea_0/(mc^2) = 0.5$. We use Eq. (4) to set the initial fluid velocities (consistent with the two fluid soliton solution) in each grid point for each species. These velocities are then interpolated to the actual positions of the particles using the same quadratic scheme applied to the charge and current densities.[41] As described above, we also add a relativistic thermal velocity for the particles, using a Lorentz transformation for the addition of velocities, obtained from a Maxwell-Jüttner distribution, Eq. (12), with $\mu = 100$.[39] We set the initial electric and magnetic fields for the simulation from the soliton solution for the vector potential given by Eq. (9), which corresponds to a left-handed circularly polarized wave. We have chosen an initial normalized wave number $ck/\Omega_c = 0.7$, and using the approximate dispersion relation for the strongly magnetized case, Eq. (5), we calculate the normalized frequency of the initial wave modulation as $\omega/\Omega_c = 0.38$. This frequency is very similar to the one obtained with the exact dispersion relation (2). Also, for the initial condition, Eq. (9), we have to choose a value for the effective group velocity of the wave packet, V/c. Fig. 3 shows the initial profile for the transverse magnetic field for $\sqrt{\lambda}a_0 = 0.5$, $\alpha = \omega_{pe}/\Omega_c = 1$, $\mu = 100$, and $V/c = 0.3$.

We let the system evolve from this initial condition until $\omega_{pe}t = 1310.72$. As we have chosen an effective group velocity of $V/c = 0.3$ for the structure, it is expected to propagate to the right. Fig. 4 shows the transverse magnetic

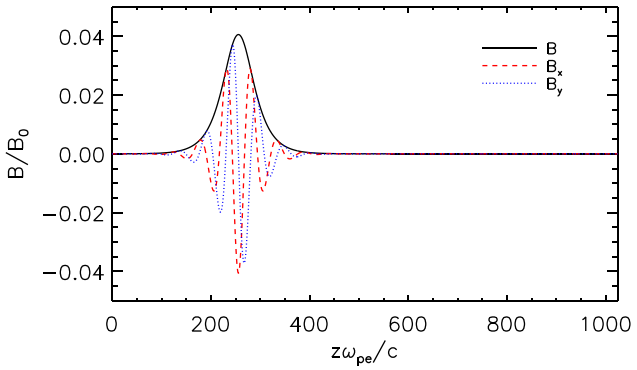

FIG. 3. Initial condition for the transverse magnetic field. Normalized magnetic field as a function of $z\omega_{pe}/c$, for $\sqrt{\lambda}a_0 = 0.5$, $\alpha = 1$, $\mu = 100$, and $V/c = 0.3$. Solid (black) line: transverse magnetic field $B/B_0 = \sqrt{B_x^2 + B_y^2}/B_0$. Dashed (red) line: B_x/B_0. Dotted (blue) line: B_y/B_0.

field profile for three different times. Fig. 4(a) shows the time $\omega_{pe}t = 249.9$. Initially, the structure splits in two wave packets propagating in opposite directions. The secondary pulse, propagating to the left, has an amplitude comparable to the amplitude of the principal pulse, propagating to the right. Both pulses continue propagating as localized structures, keeping an almost constant profile. Given the periodic boundary conditions, the pulse propagating to the left reaches the origin and appears at the other end of the simulation box, as it can be seen in Fig. 4(b) for $\omega_{pe}t = 600$. Because pulses propagate in opposite directions, they eventually collide, in this case at $\omega_{pe}t \approx 900$ (see Fig. 5). Fig. 4(c) shows the pulses profile at $\omega_{pe}t = 1150.7$, once the collision has already occurred. We can see that both pulses propagate with the same profile they had before the collision, as in Fig. 4(b), exhibiting a typical soliton-like behavior. Therefore, the envelope soliton solution obtained from the relativistic fluid model in the strongly magnetized limit does not propagate as a single soliton-like solution in the simulation. This is not surprising since we use an approximate two fluid solution in a PIC simulation. The system evolves in such a way that the envelope soliton splits in two pulses propagating in opposite directions. These pulses seem to be stable solutions of the system, since they propagate as localized structures, with a constant velocity and spatial profile, even after they collide with each other. This splitting of the initial soliton has been reported in the previous works using hybrid simulations and MHD equations for derivative nonlinear Schrödinger (DNLS) solutions, in electron-ion plasmas;[28,29] however, the authors do not allow the two structures to interact. This soliton-like behavior is an interesting result that appears in the PIC simulation and should serve as a more realistic approximation to localized structures that are stable even under kinetic considerations.

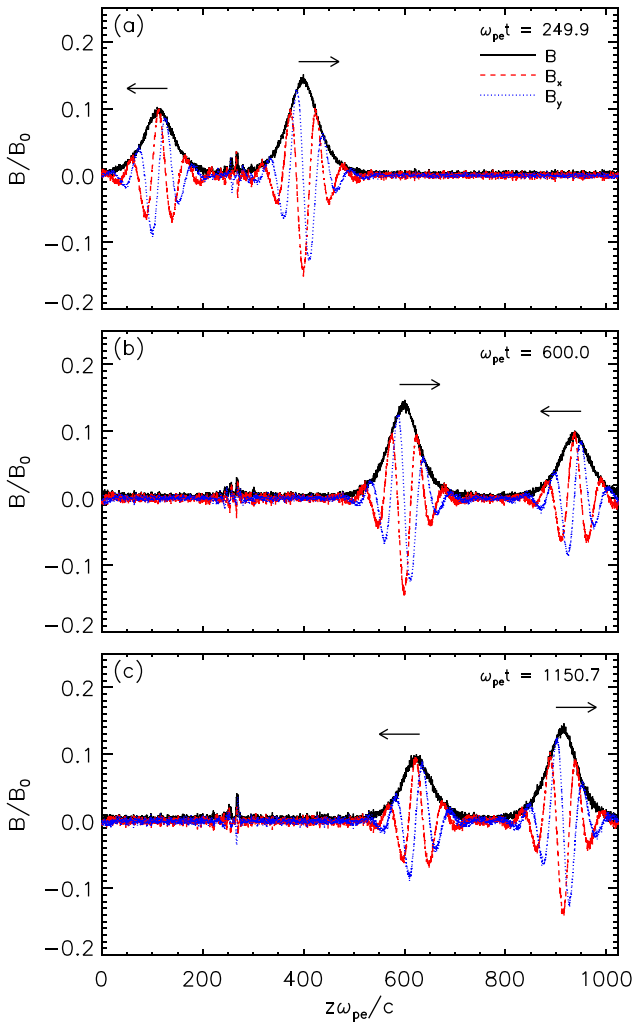

FIG. 4. Temporal evolution of the magnetic field for $\sqrt{\lambda}a_0 = 0.5$, $\alpha = 1$, $\mu = 100$, and $V/c = 0.3$. (a) $\omega_{pe}t = 249.9$, (b) $\omega_{pe}t = 600$, (c) $\omega_{pe}t = 1150.7$. Solid (black) line: transverse magnetic field B/B_0. Dashed (red) line: B_x/B_0. Dotted (blue) line: B_y/B_0. Arrows indicate the direction of propagation.

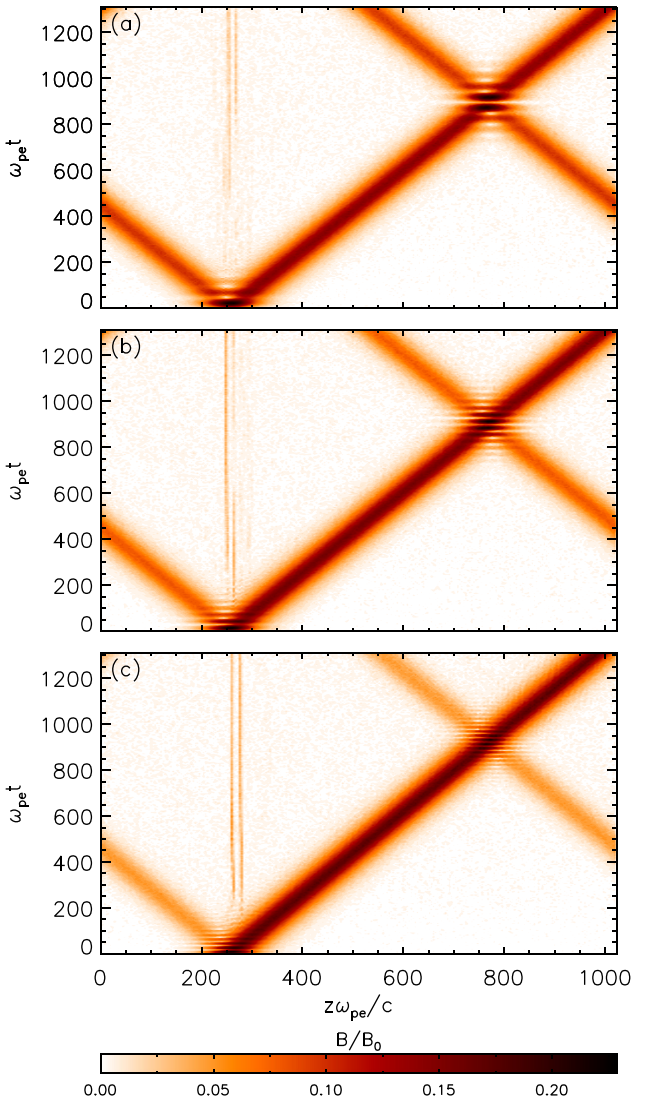

FIG. 5. Spatio-temporal evolution of the transverse magnetic field for $\sqrt{\lambda}a_0 = 0.5$, $\alpha = 1$, and $\mu = 100$. (a) $V/c = 0.3$, (b) $V/c = 0.5$, (c) $V/c = 0.8$.

Figure 5 shows the spatio-temporal evolution of the transverse magnetic field $B/B_0 = \sqrt{B_x^2 + B_y^2}/B_0$ in the $\omega_{pe}t$ vs. $z\omega_{pe}/c$ plane for $\sqrt{\lambda}a_0 = 0.5$, $\alpha = 1$, $\mu = 100$, and several group velocities V/c. The color palette shows the amplitude of the normalized magnetic field. In Fig. 5(a), we show the same case of Fig. 4, $V/c = 0.3$. We can see clearly that the

color in the two pulses remains almost equal during the entire period of simulation, which means that the spatial profile remains quite constant, even after they cross each other. There is a variation in the amplitude of the pulses at the beginning of the simulation and at $\omega_{pe}t \approx 900$, when the pulses interact. From this figure, we can also see that both pulses propagate at equal and constant velocities, approximately $v_p/c \approx 0.56$. This velocity does not match the effective group velocity given in the initial condition, V/c. Although, the amplitude of the localized structures is clearly different, their propagating speed is the same, so that—as also seen in Section IV—the commonly accepted view of an amplitude dependent velocity does not apply for these localized structures, at least in the parameter region studied here. Figs. 5(b) and 5(c) show the cases $V/c = 0.5$ and $V/c = 0.8$, respectively. We note that as we increase the group velocity V/c in the initial condition, the second pulse (propagating to the left) decreases its amplitude, whereas the principal pulse increases its amplitude.

We can see that there is a residual magnetic field fluctuation in Fig. 5(a) at $z\omega_{pe}/c = 250$ during the entire simulation. This residual magnetic field is located at the position of the original structure, where it is separated in two pulses. For larger group velocities, the residual magnetic fluctuations at $z\omega_{pe}/c \approx 250$ evolve into two localized structures that do not propagate in space, as can be seen by the formation of two vertical lines in Fig. 5(c).

Again from these figures, it is clear that the propagation velocity of the pulses does not depend on the initial group velocity, V/c. This parameter only affects the number of modes within the initial wave packet. On the other hand, the velocity of the localized structures decreases slightly with temperature as can be seen in Fig. 6, where we show the same case of Fig. 5(c), but for larger temperatures: $\mu = 50$ in Fig. 5(a) and $\mu = 10$ in Fig. 5(b). As we increase the relativistic temperature, the residual stationary structure observed in Figs. 5(a)–5(c) and 6(a) is absorbed by the thermal noise.

VI. CONCLUSIONS

We have studied the long term evolution of a left-handed spatially homogeneous circularly polarized Alfvén wave propagating parallel to the background magnetic field in a relativistic electron-positron plasma with finite temperatures, using a PIC code. We choose a large enough pump wave amplitude to accentuate the nonlinear effects, but staying in the magnetized limit $\omega/\Omega_c < 1$ regime. The evolution of this parallel propagating wave leads to the formation of localized pulses propagating antiparallel to the background magnetic field, and with an amplitude independent velocity, suggesting that this system supports soliton-like structures, and that these localized structures seem to be the naturally stable long term nonlinear solutions of the system, long after the parametric perturbation evolves.

We have also studied the spatio-temporal evolution of an initial envelope two fluid soliton solution of nonlinear Schrödinger equation derived from a relativistic two fluid system, in a strongly magnetized ($\omega \ll \Omega_c$) electron-positron plasma with relativistic temperatures, using a full particle-in-

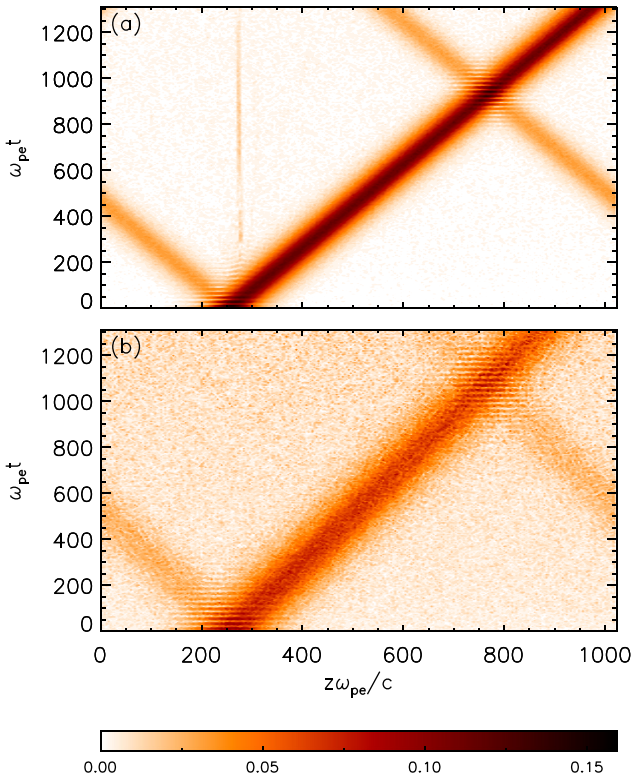

FIG. 6. Spatio-temporal evolution of the transverse magnetic field for $\sqrt{\lambda}a_0 = 0.5$, $\alpha = 1$, and $V/c = 0.8$. (a) $\mu = 50$ and (b) $\mu = 10$.

cell simulation. The initial condition for the envelope soliton solution is set consistently with the transverse velocity for each particle species. This solution turns out not to be stable in the simulation, instead, the fluid envelope soliton splits into two localized structures that propagate in opposite directions. Given the spatial periodic boundary conditions, at some point, $\omega_{pe}t \approx 900$, these two pulses collide. After the collision, the profile of the pulses remain almost unaffected, which is a typical soliton-like behavior. Both pulses propagate at the same velocity, $v_p/c \approx 0.56$, despite the fact that they have different amplitudes, which does not follow the standard view of NLS-type solitons. Furthermore, this velocity does not depend on the initial effective group velocity V/c, but it does depend on the temperature. The group velocity V does affect the relative amplitude of the pulses, with the one propagating to the left being smaller when the effective group velocity is larger.

The initial two fluid envelope soliton solution is not stable in the simulation, which is not strange if we note that the solution is an approximate result in the strongly magnetized regime, in the context of a relativistic two fluid theory, and we would not, necessarily, expect it to be an exact solution of the fully kinetic system. However, we note that by evolving this initial condition, the system leads to the formation of localized structures propagating with constant velocity and profile, independent of their amplitude, even after they collide each other (as the periodic boundary condition allows the encounter of the structures). This behavior suggests that the long term evolution of relativistic electron-positron plasmas includes stable localized structures.

These results may be relevant in the study of electromagnetic waves propagation in environments where electron-positron plasmas and strong magnetic fields are important, such as the wave propagation in pulsar magnetospheres,[5] relativistic jets,[33] and quasars,[34] among others.

ACKNOWLEDGMENTS

We thank the support of CONICyT through FONDECyT Grants Nos. 1150718 and 1130273 (J.A.V.); No. 1121144 (V.M.); and Postdoctoral Grant No. 3140142. (R.A.L.). We also thank financial support from CEDENNA. A.F.V. would like to thank the NASA-Wind/SWE project for their support.

[1]G. Björnsson, M. A. Abramowicz, X. Chen, and J.-P. Lasota, Astrophys. J. **467**, 99 (1996).
[2]E. P. T. Liang, Astrophys. J. **234**, 1105 (1979).
[3]T. R. White and A. P. Lightman, Astrophys. J. **340**, 1024 (1989).
[4]M. F. Curtis, *The Theory of Neutron Stars Magnetospheres* (University of Chicago Press, Chicago, 1991).
[5]Y. N. Istomin and D. N. Sobyanin, Astron. Lett. **33**, 660 (2007).
[6]*The Very Early Universe*, edited by G. W. Gibbons, S. Hawking, and S. T. C. Siklos (Cambridge University Press, Cambridge, 1985).
[7]T. Tajima and T. Taniuti, Phys. Rev. A **42**, 3587 (1990).
[8]D. B. Blaschke, A. V. Prozorkevich, C. D. Roberts, S. M. Schmidt, and S. A. Smolyansky, Phys. Rev. Lett. **96**, 140402 (2006).
[9]H. Chen, S. C. Wilks, J. D. Bonlie, E. P. Liang, J. Myatt, D. F. Price, D. D. Meyerhofer, and P. Beiersdorfer, Phys. Rev. Lett. **102**, 105001 (2009).
[10]G. Sarri *et al.*, Nat. Commun. **6**, 6747 (2015).
[11]P. Helander and D. J. Ward, Phys. Rev. Lett. **90**, 135004 (2003).
[12]A. C.-L. Chian and C. F. Kennel, Astrophys. Space Sci. **97**, 9 (1983).
[13]F. Verheest, Phys. Plasmas **13**, 082301 (2006).
[14]A. E. Dubinov, I. D. Dubinova, and V. A. Gordienko, Phys. Plasmas **13**, 082111 (2006).
[15]M. Nopoush and H. Abbasi, Phys. Plasmas **18**, 082106 (2011).
[16]X. Qi, Y. Xu, W. Duan, L. Zhang, and L. Yang, Phys. Plasmas **21**, 082118 (2014).
[17]O. Pezzi, F. Valentini, and P. Veltri, Eur. Phys. J. D **68**, 128 (2014).
[18]B. Eliasson and P. K. Shukla, Phys. Rev. E **71**, 046402 (2005).
[19]C. S. Jao and L. N. Hau, Phys. Rev. E **86**, 056401 (2012).
[20]C. S. Jao and L. N. Hau, Phys. Rev. E **89**, 053104 (2014).
[21]M. Y. Yu, P. K. Shukla, and L. Stenflo, Astrophys. J. **309**, L63 (1986).
[22]F. B. Rizatto, R. S. Schneider, and D. Dillenburg, Phys. Lett. A **133**, 59 (1988).
[23]E. Asseo and A. Riazuelo, Mon. Not. R. Astron. Soc. **318**, 983 (2000).
[24]V. I. Berezhiani, S. M. Mahajan, Z. Yoshida, and M. Ohhashi, Phys. Rev. E **65**, 047402 (2002).
[25]T. Cattaert, I. Kourakis, and P. K. Shukla, Phys. Plasmas **12**, 012319 (2005).
[26]F. A. Asenjo, F. Borotto, A. C.-L. Chian, V. Muñoz, J. A. Valdivia, and E. Rempel, Phys. Rev. E **85**, 046406 (2012).
[27]R. A. López, F. Asenjo, V. Muñoz, A. C.-L. Chian, and J. A. Valdivia, Phys. Rev. E **88**, 023105 (2013).
[28]B. Buti, V. Jayanti, A. F. Viñas, S. Ghosh, M. L. Goldstein, D. A. Roberts, G. S. Lakhina, and B. T. Tsurutani, Geophys. Res. Lett. **25**, 2377, doi:10.1029/98GL01688 (1998).
[29]B. Buti, M. Velli, P. C. Liewer, B. E. Goldstein, and T. Hada, Phys. Plasmas **7**, 3998 (2000).
[30]R. A. López, V. Muñoz, A. F. Viñas, and J. A. Valdivia, Phys. Plasmas **21**, 032102 (2014).
[31]R. A. López, P. S. Moya, V. Muñoz, A. Viñas, and J. A. Valdivia, Phys. Plasmas **21**, 092107 (2014).
[32]R. A. López, R. E. Navarro, P. S. Moya, A. F. Viñas, J. A. Araneda, V. Muñoz, and J. A. Valdivia, "Spontaneous electromagnetic fluctuations in a relativistic magnetized electron-positron plasma," Astrophys. J. **810**, 103 (2015).
[33]S. Iwamoto and F. Takahara, Astrophys. J. **565**, 163 (2002).
[34]J. F. C. Wardle, D. C. Homan, R. Ojha, and D. H. Roberts, Nature **395**, 457 (1998).
[35]F. A. Asenjo, V. Muñoz, J. A. Valdivia, and T. Hada, Phys. Plasmas **16**, 122108 (2009).
[36]F. A. Asenjo, V. Muñoz, and J. A. Valdivia, Phys. Rev. E **81**, 056405 (2010).
[37]R. A. López, F. A. Asenjo, V. Muñoz, and J. A. Valdivia, Phys. Plasmas **19**, 082104 (2012).
[38]K. Nishikawa and C. S. Liu, in *Advances in Plasma Physics*, edited by A. Simon and W. B. Thompson (Wiley, New York, 1976), Vol. 6, Chap. 2, pp. 3–81.
[39]F. Jüttner, Ann. Phys. **339**, 856 (1911).
[40]P. L. Pritchett, Space Sci. Rev. **42**, 17 (1985).
[41]C. K. Birdsall and A. B. Langdon, *Plasma Physics Via Computer Simulation* (Taylor and Francis, New York, 2005).
[42]H. Matsumoto and Y. Omura, *Computer Space Plasma Physics: Simulation Techniques and Software* (Terra Scientific, Tokyo, 1993).
[43]*Advanced Methods for Space Simulations*, edited by H. Usui and Y. Omura (Terra Scientific, Tokyo, 2007).
[44]J. P. Verboncoeur, Plasma Phys. Controlled Fusion **47**, A231 (2005).
[45]B. Marder, J. Comput. Phys. **68**, 48 (1987).
[46]A. B. Langdon, Comput. Phys. Commun. **70**, 447 (1992).
[47]H. L. Pecseli, *Waves and Oscillations in Plasmas, Series in Plasma Physics* (CRC Press, Hoboken, NJ, 2012).